FERMILAB-PUB-19-253-E *Published in Phys. Rev. D as DOI: 10.1103/PhysRevD.100.012005*

Properties of $Z_c^{\pm}(3900)$ produced in $p\bar{p}$ collisions

V.M. Abazov,[31] B. Abbott,[67] B.S. Acharya,[25] M. Adams,[46] T. Adams,[44] J.P. Agnew,[41] G.D. Alexeev,[31] G. Alkhazov,[35] A. Alton[a],[56] A. Askew,[44] S. Atkins,[54] K. Augsten,[7] V. Aushev,[38] Y. Aushev,[38] C. Avila,[5] F. Badaud,[10] L. Bagby,[45] B. Baldin,[45] D.V. Bandurin,[74] S. Banerjee,[25] E. Barberis,[55] P. Baringer,[53] J.F. Bartlett,[45] U. Bassler,[15] V. Bazterra,[46] A. Bean,[53] M. Begalli,[2] L. Bellantoni,[45] S.B. Beri,[23] G. Bernardi,[14] R. Bernhard,[19] I. Bertram,[39] M. Besançon,[15] R. Beuselinck,[40] P.C. Bhat,[45] S. Bhatia,[58] V. Bhatnagar,[23] G. Blazey,[47] S. Blessing,[44] K. Bloom,[59] A. Boehnlein,[45] D. Boline,[64] E.E. Boos,[33] G. Borissov,[39] M. Borysova[l],[38] A. Brandt,[71] O. Brandt,[20] M. Brochmann,[75] R. Brock,[57] A. Bross,[45] D. Brown,[14] X.B. Bu,[45] M. Buehler,[45] V. Buescher,[21] V. Bunichev,[33] S. Burdin[b],[39] C.P. Buszello,[37] E. Camacho-Pérez,[28] B.C.K. Casey,[45] H. Castilla-Valdez,[28] S. Caughron,[57] S. Chakrabarti,[64] K.M. Chan,[51] A. Chandra,[73] E. Chapon,[15] G. Chen,[53] S.W. Cho,[27] S. Choi,[27] B. Choudhary,[24] S. Cihangir[‡],[45] D. Claes,[59] J. Clutter,[53] M. Cooke[j],[45] W.E. Cooper,[45] M. Corcoran[‡],[73] F. Couderc,[15] M.-C. Cousinou,[12] J. Cuth,[21] D. Cutts,[70] A. Das,[72] G. Davies,[40] S.J. de Jong,[29,30] E. De La Cruz-Burelo,[28] F. Déliot,[15] R. Demina,[63] D. Denisov,[65] S.P. Denisov,[34] S. Desai,[45] C. Deterre[c],[41] K. DeVaughan,[59] H.T. Diehl,[45] M. Diesburg,[45] P.F. Ding,[41] A. Dominguez,[59] A. Drutskoy[q],[32] A. Dubey,[24] L.V. Dudko,[33] A. Duperrin,[12] S. Dutt,[23] M. Eads,[47] D. Edmunds,[57] J. Ellison,[43] V.D. Elvira,[45] Y. Enari,[14] H. Evans,[49] A. Evdokimov,[46] V.N. Evdokimov,[34] A. Fauré,[15] L. Feng,[47] T. Ferbel,[63] F. Fiedler,[21] F. Filthaut,[29,30] W. Fisher,[57] H.E. Fisk,[45] M. Fortner,[47] H. Fox,[39] J. Franc,[7] S. Fuess,[45] P.H. Garbincius,[45] A. Garcia-Bellido,[63] J.A. García-González,[28] V. Gavrilov,[32] W. Geng,[12,57] C.E. Gerber,[46] Y. Gershtein,[60] G. Ginther,[45] O. Gogota,[38] G. Golovanov,[31] P.D. Grannis,[64] S. Greder,[16] H. Greenlee,[45] G. Grenier,[17] Ph. Gris,[10] J.-F. Grivaz,[13] A. Grohsjean[c],[15] S. Grünendahl,[45] M.W. Grünewald,[26] T. Guillemin,[13] G. Gutierrez,[45] P. Gutierrez,[67] J. Haley,[68] L. Han,[4] K. Harder,[41] A. Harel,[63] J.M. Hauptman,[52] J. Hays,[40] T. Head,[41] T. Hebbeker,[18] D. Hedin,[47] H. Hegab,[68] A.P. Heinson,[43] U. Heintz,[70] C. Hensel,[1] I. Heredia-De La Cruz[d],[28] K. Herner,[45] G. Hesketh[f],[41] M.D. Hildreth,[51] R. Hirosky,[74] T. Hoang,[44] J.D. Hobbs,[64] B. Hoeneisen,[9] J. Hogan,[73] M. Hohlfeld,[21] J.L. Holzbauer,[58] I. Howley,[71] Z. Hubacek,[7,15] V. Hynek,[7] I. Iashvili,[62] Y. Ilchenko,[72] R. Illingworth,[45] A.S. Ito,[45] S. Jabeen[m],[45] M. Jaffré,[13] A. Jayasinghe,[67] M.S. Jeong,[27] R. Jesik,[40] P. Jiang[‡],[4] K. Johns,[42] E. Johnson,[57] M. Johnson,[45] A. Jonckheere,[45] P. Jonsson,[40] J. Joshi,[43] A.W. Jung[o],[45] A. Juste,[36] E. Kajfasz,[12] D. Karmanov,[33] I. Katsanos,[59] M. Kaur,[23] R. Kehoe,[72] S. Kermiche,[12] N. Khalatyan,[45] A. Khanov,[68] A. Kharchilava,[62] Y.N. Kharzheev,[31] I. Kiselevich,[32] J.M. Kohli,[23] A.V. Kozelov,[34] J. Kraus,[58] A. Kumar,[62] A. Kupco,[8] T. Kurča,[17] V.A. Kuzmin,[33] S. Lammers,[49] P. Lebrun,[17] H.S. Lee,[27] S.W. Lee,[52] W.M. Lee[‡],[45] X. Lei,[42] J. Lellouch,[14] D. Li,[14] H. Li,[74] L. Li,[43] Q.Z. Li,[45] J.K. Lim,[27] D. Lincoln,[45] J. Linnemann,[57] V.V. Lipaev[‡],[34] R. Lipton,[45] H. Liu,[72] Y. Liu,[4] A. Lobodenko,[35] M. Lokajicek,[8] R. Lopes de Sa,[45] R. Luna-Garcia[g],[28] A.L. Lyon,[45] A.K.A. Maciel,[1] R. Madar,[19] R. Magaña-Villalba,[28] S. Malik,[59] V.L. Malyshev,[31] J. Mansour,[20] J. Martínez-Ortega,[28] R. McCarthy,[64] C.L. McGivern,[41] M.M. Meijer,[29,30] A. Melnitchouk,[45] D. Menezes,[47] P.G. Mercadante,[3] M. Merkin,[33] A. Meyer,[18] J. Meyer[i],[20] F. Miconi,[16] N.K. Mondal,[25] M. Mulhearn,[74] E. Nagy,[12] M. Narain,[70] R. Nayyar,[42] H.A. Neal[‡],[56] J.P. Negret,[5] P. Neustroev,[35] H.T. Nguyen,[74] T. Nunnemann,[22] J. Orduna,[70] N. Osman,[12] A. Pal,[71] N. Parashar,[50] V. Parihar,[70] S.K. Park,[27] R. Partridge[e],[70] N. Parua,[49] A. Patwa[j],[65] B. Penning,[40] M. Perfilov,[33] Y. Peters,[41] K. Petridis,[41] G. Petrillo,[63] P. Pétroff,[13] M.-A. Pleier,[65] V.M. Podstavkov,[45] A.V. Popov,[34] M. Prewitt,[73] D. Price,[41] N. Prokopenko,[34] J. Qian,[56] A. Quadt,[20] B. Quinn,[58] P.N. Ratoff,[39] I. Razumov,[34] I. Ripp-Baudot,[16] F. Rizatdinova,[68] M. Rominsky,[45] A. Ross,[39] C. Royon,[8] P. Rubinov,[45] R. Ruchti,[51] G. Sajot,[11] A. Sánchez-Hernández,[28] M.P. Sanders,[22] A.S. Santos[h],[1] G. Savage,[45] M. Savitskyi,[38] L. Sawyer,[54] T. Scanlon,[40] R.D. Schamberger,[64] Y. Scheglov[‡],[35] H. Schellman,[69,48] M. Schott,[21] C. Schwanenberger,[41] R. Schwienhorst,[57] J. Sekaric,[53] H. Severini,[67] E. Shabalina,[20] V. Shary,[15] S. Shaw,[41] A.A. Shchukin,[34] O. Shkola,[38] V. Simak,[7] P. Skubic,[67] P. Slattery,[63] G.R. Snow[‡],[59] J. Snow,[66] S. Snyder,[65] S. Söldner-Rembold,[41] L. Sonnenschein,[18] K. Soustruznik,[6] J. Stark,[11] N. Stefaniuk,[38] D.A. Stoyanova,[34] M. Strauss,[67] L. Suter,[41] P. Svoisky,[74] M. Titov,[15] V.V. Tokmenin,[31] Y.-T. Tsai,[63] D. Tsybychev,[64] B. Tuchming,[15] C. Tully,[61] L. Uvarov,[35] S. Uvarov,[35] S. Uzunyan,[47] R. Van Kooten,[49] W.M. van Leeuwen,[29] N. Varelas,[46] E.W. Varnes,[42] I.A. Vasilyev,[34] A.Y. Verkheev,[31] L.S. Vertogradov,[31] M. Verzocchi,[45] M. Vesterinen,[41] D. Vilanova,[15] P. Vokac,[7] H.D. Wahl,[44] M.H.L.S. Wang,[45] J. Warchol[‡],[51] G. Watts,[75] M. Wayne,[51] J. Weichert,[21] L. Welty-Rieger,[48] M.R.J. Williams[n],[49] G.W. Wilson,[53] M. Wobisch,[54] D.R. Wood,[55] T.R. Wyatt,[41] Y. Xie,[45] R. Yamada,[45] S. Yang,[4] T. Yasuda,[45] Y.A. Yatsunenko,[31] W. Ye,[64] Z. Ye,[45] H. Yin,[45] K. Yip,[65] S.W. Youn,[45] J.M. Yu,[56]

J. Zennamo,[62] T.G. Zhao,[41] B. Zhou,[56] J. Zhu,[56] M. Zielinski,[63] D. Zieminska,[49] and L. Zivkovic[p14]
(The D0 Collaboration*)
[1]LAFEX, Centro Brasileiro de Pesquisas Físicas, Rio de Janeiro, RJ 22290, Brazil
[2]Universidade do Estado do Rio de Janeiro, Rio de Janeiro, RJ 20550, Brazil
[3]Universidade Federal do ABC, Santo André, SP 09210, Brazil
[4]University of Science and Technology of China, Hefei 230026, People's Republic of China
[5]Universidad de los Andes, Bogotá, 111711, Colombia
[6]Charles University, Faculty of Mathematics and Physics, Center for Particle Physics, 116 36 Prague 1, Czech Republic
[7]Czech Technical University in Prague, 116 36 Prague 6, Czech Republic
[8]Institute of Physics, Academy of Sciences of the Czech Republic, 182 21 Prague, Czech Republic
[9]Universidad San Francisco de Quito, Quito 170157, Ecuador
[10]LPC, Université Blaise Pascal, CNRS/IN2P3, Clermont, F-63178 Aubière Cedex, France
[11]LPSC, Université Joseph Fourier Grenoble 1, CNRS/IN2P3, Institut National Polytechnique de Grenoble, F-38026 Grenoble Cedex, France
[12]CPPM, Aix-Marseille Université, CNRS/IN2P3, F-13288 Marseille Cedex 09, France
[13]LAL, Univ. Paris-Sud, CNRS/IN2P3, Université Paris-Saclay, F-91898 Orsay Cedex, France
[14]LPNHE, Universités Paris VI and VII, CNRS/IN2P3, F-75005 Paris, France
[15]CEA Saclay, Irfu, SPP, F-91191 Gif-Sur-Yvette Cedex, France
[16]IPHC, Université de Strasbourg, CNRS/IN2P3, F-67037 Strasbourg, France
[17]IPNL, Université Lyon 1, CNRS/IN2P3, F-69622 Villeurbanne Cedex, France and Université de Lyon, F-69361 Lyon CEDEX 07, France
[18]III. Physikalisches Institut A, RWTH Aachen University, 52056 Aachen, Germany
[19]Physikalisches Institut, Universität Freiburg, 79085 Freiburg, Germany
[20]II. Physikalisches Institut, Georg-August-Universität Göttingen, 37073 Göttingen, Germany
[21]Institut für Physik, Universität Mainz, 55099 Mainz, Germany
[22]Ludwig-Maximilians-Universität München, 80539 München, Germany
[23]Panjab University, Chandigarh 160014, India
[24]Delhi University, Delhi-110 007, India
[25]Tata Institute of Fundamental Research, Mumbai-400 005, India
[26]University College Dublin, Dublin 4, Ireland
[27]Korea Detector Laboratory, Korea University, Seoul, 02841, Korea
[28]CINVESTAV, Mexico City 07360, Mexico
[29]Nikhef, Science Park, 1098 XG Amsterdam, the Netherlands
[30]Radboud University Nijmegen, 6525 AJ Nijmegen, the Netherlands
[31]Joint Institute for Nuclear Research, Dubna 141980, Russia
[32]Institute for Theoretical and Experimental Physics, Moscow 117259, Russia
[33]Moscow State University, Moscow 119991, Russia
[34]Institute for High Energy Physics, Protvino, Moscow region 142281, Russia
[35]Petersburg Nuclear Physics Institute, St. Petersburg 188300, Russia
[36]Institució Catalana de Recerca i Estudis Avançats (ICREA) and Institut de Física d'Altes Energies (IFAE), 08193 Bellaterra (Barcelona), Spain
[37]Uppsala University, 751 05 Uppsala, Sweden
[38]Taras Shevchenko National University of Kyiv, Kiev, 01601, Ukraine
[39]Lancaster University, Lancaster LA1 4YB, United Kingdom
[40]Imperial College London, London SW7 2AZ, United Kingdom
[41]The University of Manchester, Manchester M13 9PL, United Kingdom
[42]University of Arizona, Tucson, Arizona 85721, USA
[43]University of California Riverside, Riverside, California 92521, USA
[44]Florida State University, Tallahassee, Florida 32306, USA
[45]Fermi National Accelerator Laboratory, Batavia, Illinois 60510, USA
[46]University of Illinois at Chicago, Chicago, Illinois 60607, USA
[47]Northern Illinois University, DeKalb, Illinois 60115, USA
[48]Northwestern University, Evanston, Illinois 60208, USA
[49]Indiana University, Bloomington, Indiana 47405, USA
[50]Purdue University Calumet, Hammond, Indiana 46323, USA
[51]University of Notre Dame, Notre Dame, Indiana 46556, USA
[52]Iowa State University, Ames, Iowa 50011, USA
[53]University of Kansas, Lawrence, Kansas 66045, USA
[54]Louisiana Tech University, Ruston, Louisiana 71272, USA
[55]Northeastern University, Boston, Massachusetts 02115, USA
[56]University of Michigan, Ann Arbor, Michigan 48109, USA
[57]Michigan State University, East Lansing, Michigan 48824, USA

[58] University of Mississippi, University, Mississippi 38677, USA
[59] University of Nebraska, Lincoln, Nebraska 68588, USA
[60] Rutgers University, Piscataway, New Jersey 08855, USA
[61] Princeton University, Princeton, New Jersey 08544, USA
[62] State University of New York, Buffalo, New York 14260, USA
[63] University of Rochester, Rochester, New York 14627, USA
[64] State University of New York, Stony Brook, New York 11794, USA
[65] Brookhaven National Laboratory, Upton, New York 11973, USA
[66] Langston University, Langston, Oklahoma 73050, USA
[67] University of Oklahoma, Norman, Oklahoma 73019, USA
[68] Oklahoma State University, Stillwater, Oklahoma 74078, USA
[69] Oregon State University, Corvallis, Oregon 97331, USA
[70] Brown University, Providence, Rhode Island 02912, USA
[71] University of Texas, Arlington, Texas 76019, USA
[72] Southern Methodist University, Dallas, Texas 75275, USA
[73] Rice University, Houston, Texas 77005, USA
[74] University of Virginia, Charlottesville, Virginia 22904, USA
[75] University of Washington, Seattle, Washington 98195, USA

(Dated: May 31, 2019)

We study the production of the exotic charged charmonium-like state $Z_c^{\pm}(3900)$ in $p\overline{p}$ collisions through the sequential process $\psi(4260) \to Z_c^{\pm}(3900)\pi^{\mp}$, $Z_c^{\pm}(3900) \to J/\psi\pi^{\pm}$. Using the subsample of candidates originating from semi-inclusive weak decays of b-flavored hadrons, we measure the invariant mass and natural width to be $M = 3902.6^{+5.2}_{-5.0}\,(\text{stat})^{+3.3}_{-1.4}\,(\text{syst})$ MeV and $\Gamma = 32^{+28}_{-21}\,(\text{stat})^{+26}_{-7}\,(\text{syst})$ MeV, respectively. We search for prompt production of the $Z_c^{\pm}(3900)$ through the same sequential process. No significant signal is observed, and we set an upper limit of 0.70 at the 95% credibility level on the ratio of prompt production to the production via b-hadron decays. The study is based on 10.4 fb^{-1} of $p\overline{p}$ collision data collected by the D0 experiment at the Fermilab Tevatron collider.

I. INTRODUCTION

In high-energy hadron collisions, charmonium is known to be produced both promptly in QCD processes and non-promptly in b-hadron decays, with well measured rates. For both J/ψ and $\psi(2S)$ mesons the non-prompt fraction increases with transverse momentum but prompt production dominates in most of the studied p_T range [1].

Much less information exists about the hadronic production of exotic multiquark states containing a charm quark and antiquark. The $X(3872)$ – the most extensively studied exotic meson – is produced copiously in prompt $p\overline{p}$ interactions at $\sqrt{s} = 1.96$ TeV [2], and in pp collisions at $\sqrt{s} = 7$ TeV [3] and $\sqrt{s} = 8$ TeV [4]. The fraction of the inclusive production rate of the $X(3872)$ mesons originating from decays of b-flavored hadrons (H_b) is found to be approximately 0.3 [3, 4], independent of p_T. Evidence for prompt production of the $X(4140)$, another exotic candidate, was also reported by D0 [5]. The large prompt production rate of the $X(3872)$ has often been used as an argument against its identification as a weakly bound charm-meson molecule; see Ref. [6] for the latest discussion.

In Ref. [7], the D0 Collaboration presented the first evidence for production of the manifestly exotic charmonium-like state $Z_c^{\pm}(3900)$ in semi-inclusive weak decays of b-flavored hadrons in events containing a non-prompt J/ψ and a pair of oppositely charged particles, assumed to be pions. That analysis considered the mass range $4.1 < M(J/\psi\pi^+\pi^-) < 4.7$ GeV that includes the $\psi(4260)$ state: $H_b \to \psi(4260) +$ anything, $\psi(4260) \to Z_c^{\pm}(3900)\pi^{\mp}$, $Z_c^{\pm}(3900) \to J/\psi\pi^{\pm}$. This article presents an extension of that study to a search for prompt production of the $Z_c^{\pm}(3900)$ through the sequential process $\psi(4260) \to Z_c^{\pm}(3900)\pi^{\mp}$, $Z_c^{\pm}(3900) \to J/\psi\pi^{\pm}$. The event sample used in this analysis is approximately 50% larger than in Ref. [7] due to the use of an extended track finding algorithm optimized for reconstructing low-p_T tracks.

---

*with visitors from [a]Augustana College, Sioux Falls, SD 57197, USA, [b]The University of Liverpool, Liverpool L69 3BX, UK, [c]Deutshes Elektronen-Synchrotron (DESY), Notkestrasse 85, Germany, [d]CONACyT, M-03940 Mexico City, Mexico, [e]SLAC, Menlo Park, CA 94025, USA, [f]University College London, London WC1E 6BT, UK, [g]Centro de Investigacion en Computacion - IPN, CP 07738 Mexico City, Mexico, [h]Universidade Estadual Paulista, São Paulo, SP 01140, Brazil, [i]Karlsruher Institut für Technologie (KIT) - Steinbuch Centre for Computing (SCC), D-76128 Karlsruhe, Germany, [j]Office of Science, U.S. Department of Energy, Washington, D.C. 20585, USA, [l]Kiev Institute for Nuclear Research (KINR), Kyiv 03680, Ukraine, [m]University of Maryland, College Park, MD 20742, USA, [n]European Orgnaization for Nuclear Research (CERN), CH-1211 Geneva, Switzerland, [o]Purdue University, West Lafayette, IN 47907, USA, [p]Institute of Physics, Belgrade, Belgrade, Serbia, and [q]P.N. Lebedev Physical Institute of the Russian Academy of Sciences, 119991, Moscow, Russia. [‡]Deceased.

II. THE D0 DETECTOR, EVENT RECONSTRUCTION, AND SELECTION

The D0 detector has a central tracking system consisting of a silicon microstrip tracker and a central fiber tracker, both located within a 1.9 T superconducting solenoidal magnet [9, 10]. A muon system, covering $|\eta| < 2$ [11], consists of a layer of tracking detectors and scintillation trigger counters in front of a central and two forward 1.8 T iron toroidal magnets, followed by two similar layers after the toroids [12]. Events used in this analysis are collected with both single-muon and dimuon triggers. Single-muon triggers require a coincidence of signals in trigger elements inside and outside the toroidal magnets. All dimuon triggers require at least one muon to have track segments after the toroid; muons in the forward region are always required to penetrate the toroid.

The minimum muon transverse momentum is 1.5 GeV. No minimum p_T requirement is applied to the muon pair, but the effective threshold is approximately 4 GeV due to the requirement for muons to penetrate the toroids, and the average value for accepted events is 10 GeV.

In $p\overline{p}$ collisions the J/ψ is produced promptly, either directly or in strong decays of higher-mass charmonium states, or non-promptly in b-hadron decays. Prompt mesons have a decay vertex consistent with the interaction point while those from the b decays are displaced on average by $\mathcal{O}(1\text{ mm})$ as a result of the long b-hadron lifetime.

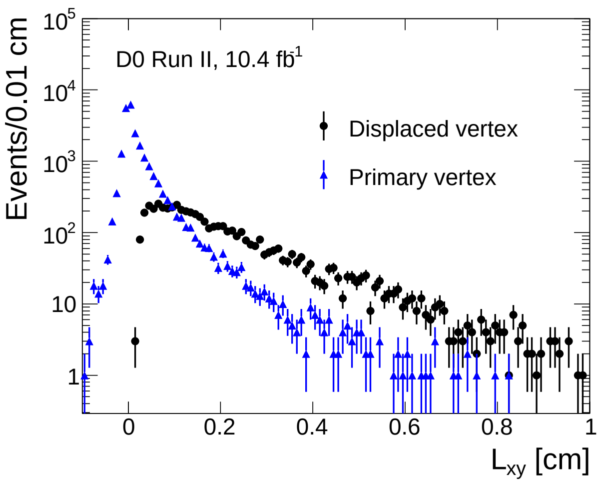

FIG. 1: The $J/\psi\pi^+\pi^-$ decay length in the transverse plane for events in the range $4.2 < M(J/\psi\pi^+\pi^-) < 4.3$ GeV. The black filled circles show the distribution of events that satisfy the criteria for a displaced vertex. This subsample constitutes about 2/3 of the nonprompt events. The distribution marked with blue triangles includes the prompt production and the remaining 1/3 of the nonprompt events.

We reconstruct $J/\psi \to \mu^+\mu^-$ decay candidates accompanied by a pair of charged particles, assumed to be pions, with opposite charges and with $p_T > 0.7$ GeV. We perform a kinematic fit under the hypothesis that the muons come from the J/ψ and that the J/ψ and the two particles originate from the same space point. In the fit, the dimuon invariant mass is constrained to the world-average value of the J/ψ meson mass [13]. The track parameters (p_T, position and direction in 3D) are readjusted according to the fit and are used in the calculation of the system's transverse decay-path vector $\vec{L}_{\rm xy}$, the invariant mass $M(J/\psi\pi^+\pi^-)$, and the masses of the two $J/\psi\pi$ subsystems. Following Refs. [14] and [15], we select the larger mass combination as a $Z_c^\pm(3900)$ candidate's mass.

We select events in the $M(J/\psi\pi^+\pi^-)$ range 4.1–4.7 GeV that includes the $\psi(4260)$ and excludes fully reconstructed decays of b hadrons to final states $J/\psi h_1^+ h_2^-$ where h_1 and h_2 stand for a pion, a kaon, or a proton. We divide the data into two non-overlapping samples: events with a displaced vertex, selected as in Ref. [7], and a complementary sample of "primary vertex" events. The criteria for the displaced vertex category are: the vertex of the J/ψ and the highest p_T track is required to be displaced in the transverse plane from the $p\bar{p}$ interaction vertex by at least 5σ, the significance of the impact parameter in the transverse plane (IP) [8] of the leading track is required to be greater than 2σ, the second track's IP significance is required to be greater than 1σ, and the second track's contribution to the J/ψ+2 tracks vertex χ^2 must be less than 6. The cosine of the angle in the transverse plane between the momentum vector and decay path of the $J/\psi + 2$ tracks system is required to be greater than 0.9.

The sample includes events where the hadronic pair comes from decays $K^* \to K\pi$ or $\phi \to KK$. We remove such events by assuming that one or both of the charged hadrons are kaons and vetoing the mass combinations $0.81 < M(\pi K) < 0.97$ GeV and $1.01 < M(KK) < 1.03$ GeV. We also veto photon conversions by removing events with $M(\pi^+\pi^-) < 0.35$ GeV. The decay-length distributions in the transverse plane for events in the "displaced vertex" and the "primary vertex" categories in the mass range $4.2 < M(J/\psi\pi^+\pi^-) < 4.3$ GeV are shown in Fig. 1.

III. $J/\psi\pi^\pm$ MASS FITS

We study the $J/\psi\pi^\pm$ system in the vicinity of the $Z_c^\pm(3900)$. We perform a binned maximum-likelihood fit of the $M(J/\psi\pi)$ distribution to a sum of a resonant signal and an incoherent background in six intervals of $M(J/\psi\pi^+\pi^-)$: 4.1–4.2 GeV, 4.2–4.3 GeV, 4.3–4.4 GeV, 4.4–4.5 GeV, 4.5–4.6 GeV, and 4.6–4.7 GeV. The signal is represented by the S-wave relativistic Breit-Wigner function convolved with a Gaussian mass resolution. The $Z_c^\pm(3900)$ mass and width are fixed to the values for the $J/\psi\pi^{\pm,0}$ channels only (see Ref. [16]): $M = 3893.3 \pm 2.7$ MeV, $\Gamma = 36.8 \pm 6.5$ MeV. The D0 mass resolution at this mass is $\sigma = 17 \pm 2$ MeV. In these fits we allow negative values for the signal yield.

For the "displaced vertex" selection, background is mainly due to weak decays of b hadrons to a J/ψ paired randomly with hadrons coming from the same multibody decay. For the "primary vertex" events, the main background is due to a promptly produced J/ψ combined with particles produced in the hadronization process. In both cases we use Chebyshev polynomials of the first kind to represent background. The fitting range limits are chosen so as to obtain an acceptable fit in a maximum range while avoiding areas where the total probability density function goes to zero. We choose the order of the Chebyshev polynomial to minimize the Akaike information test (AIC) [17]. For a fit with p free parameters to a distribution in n bins the AIC is defined as $AIC = \chi^2 + 2p + 2p(p+1)/(n-p-1)$. For the displaced-vertex subsample we choose a 4th-order polynomial, and for the "primary vertex" sample the choice is a 5th-order polynomial.

IV. FIT RESULTS

The results of the fits are shown in Figs. 2 and 3 and summarized in Table I and in Fig. 4. The statistical significance of the signal is defined as $S = \sqrt{-2\ln(\mathcal{L}_0/\mathcal{L}_{\rm max})}$, where $\mathcal{L}_{\rm max}$ and $\mathcal{L}_0$ are likelihood values at the best-fit signal yield and the signal yield fixed to zero. In the case of a negative signal yield, S corresponds to the statisical significance of the depletion.

For the "displaced-vertex" subsample we see a clear enhancement near the $Z_c^{\pm}(3900)$ mass for events in the range $4.2 < M(J/\psi\pi^+\pi^-) < 4.3$ GeV, consistent with coming from the $\psi(4260)$ which has a mass of 4230 ± 8 MeV [13], and a smaller excess in the ranges 4.5–4.6 GeV and 4.6–4.7 GeV. In the mass interval 4.3–4.4 GeV (and to smaller extent for 4.4–4.5 GeV) our fits show a negative, but not significant, yield of $Z_c^{\pm}(3900)$ events. There is no significant signal in the "primary vertex" subsamples in any $M(J/\psi\pi^+\pi^-)$ interval.

For the "displaced-vertex events" in the mass range $4.2 < M(J/\psi\pi^+\pi^-) < 4.3$ GeV we also perform a fit allowing the signal mass and width to vary. From this fit, shown in Fig. 5, we obtain our best measurement of the $Z_c^{\pm}(3900)$ signal: $M = 3902.6^{+5.2}_{-5.0}$ MeV, $\Gamma = 32^{+28}_{-21}$ MeV. The signal yield is $N = 364 \pm 156$ events, the fit quality is $\chi^2/ndf = 24.1/14$, and the statistical significance is $S = 5.4\sigma$.

V. ACCEPTANCE OF THE DISPLACED-VERTEX SELECTION

We obtain the acceptance of the "displaced-vertex" selection for H_b decay events leading to $Z_c^{\pm}(3900)$ using candidates for the decay $B_d^0 \to J/\psi K^{\pm}\pi^{\mp}$, assuming that the distributions of the decay length and its uncertainty for the B_d^0 decay are a good representation for the average b hadron. Events are required to satisfy the same kinematic and quality cuts as applied above. We find the fitted numbers of B_d^0 decays $N_{\rm displaced} = 12951 \pm 167$ and $N_{\rm primary} = 6616 \pm 162$, respectively. The ratios of $N_{\rm primary}$ to $N_{\rm displaced}$ for B_d^0 and $Z_c^{\pm}(3900)$ events with the same topology should be the same, to the extent that the lifetimes of B_d^0 and H_b are the same. With the systematic uncertainty discussed in the next section taken into account, the acceptance of the displaced vertex selection is $A = 0.66 \pm 0.02$.

VI. SYSTEMATIC UNCERTAINTIES

A. Mass and width

We assign an asymmetric systematic uncertainty of $(0, +3)$ MeV to the mass measurement due to a bias in mass measurements of b hadrons at D0. We assign the uncertainty on the mass and width due to uncertainty in the mass resolution as half of the difference of the results obtained by changing the resolution by $\pm 1\sigma$ to 15 MeV and 19 MeV. We assign uncertainties due to the background shape based on the differences in the results using the 3rd, 4th, and 5th-order polynomial. The systematic uncertainties are summarized in Table II.

B. Signal yields

The uncertainty in the relative yields of prompt and nonprompt production of the $Z_c^{\pm}(3900)$ is dominated by statistical uncertainties. The systematic uncertainties are evaluated as follows.

- Mass resolution

  We assign the uncertainty in the signal yields due to uncertainty in the mass resolution as half of the difference of the results obtained by changing the resolution by $\pm 1\sigma$ to 15 MeV and 19 MeV.

- Trigger bias

  Some of the single-muon triggers include a trigger term requiring the presence of tracks with nonzero impact parameter. Events recorded solely by such triggers constitute approximately 5% of all events. We assign a systematic uncertainty of $\pm 5\%$ to $N_{\rm displaced}$ due to this effect.

- Acceptance of the displaced-vertex selection

  Our assumption of the equality of the displaced-vertex selection acceptance for the non-prompt $Z_c^{\pm}(3900)$ and for B_d^0 is based on expectation of the equality of the average lifetime of b-hadron parents of the $Z_c^{\pm}(3900)$ and that of the B_d^0. The world-average of the B_d^0 lifetime is 3% lower than the lifetime averaged over all b hadron species [13]. This

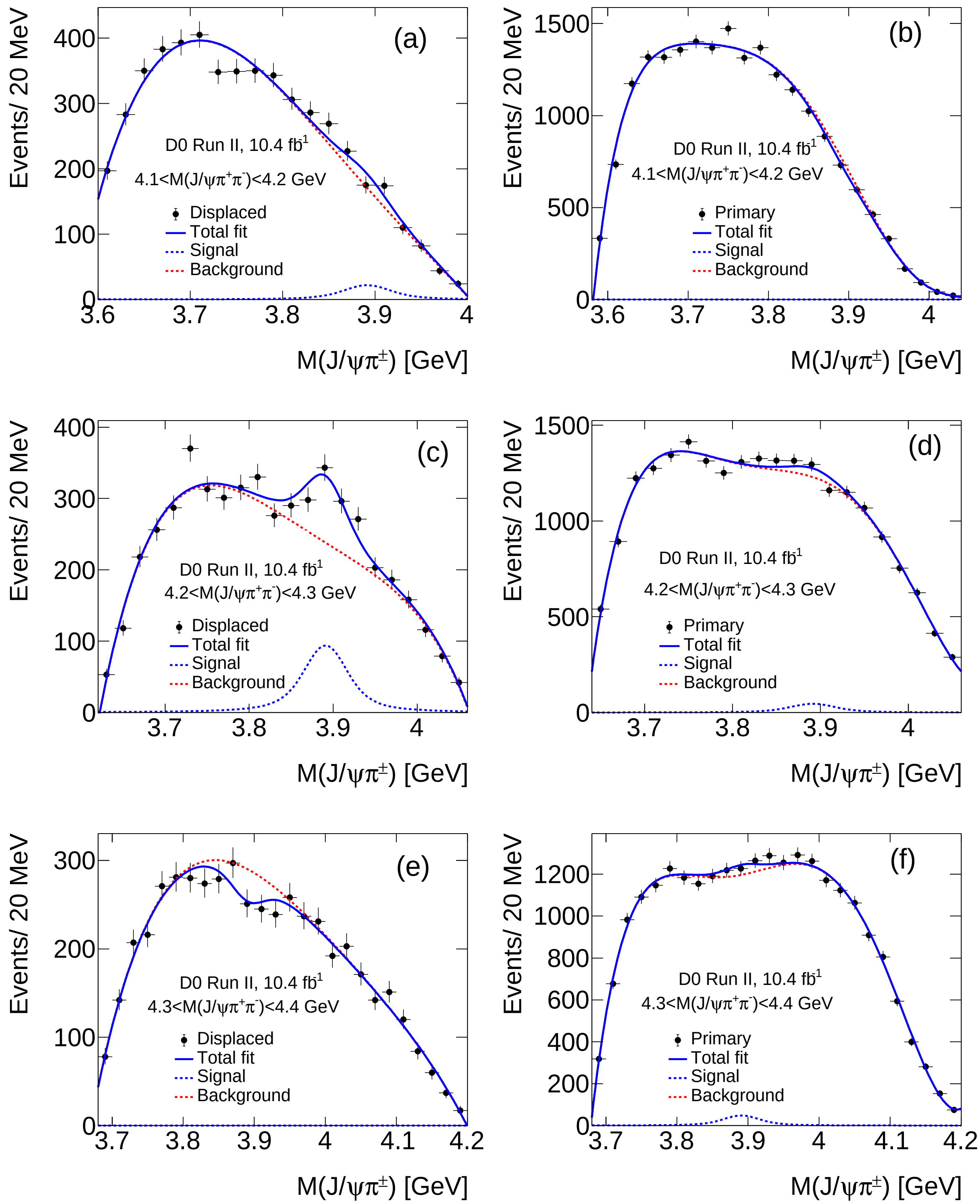

FIG. 2: The invariant mass distribution of $J/\psi\pi^{\pm}$ candidates in three intervals of $M(J/\psi\pi^+\pi^-)$, from top to bottom 4.1–4.2 GeV, 4.2–4.3 GeV, and 4.3–4.4 GeV. Left: events with a displaced vertex. Right: "primary vertex" events. Superimposed are the fits of a Breit-Wigner signal with fixed mass and width [16] (dashed blue lines), a Chebyshev polynomial background (dashed red lines), and their sum (solid blue lines).

difference corresponds to a 1% difference in the acceptance. In addition, there may be small differences between different channels in the transverse momentum distributions of the parent b hadrons and of the final-state particles. When the decay $B_s^0 \to J/\psi\phi$ is used to estimate the "displaced-vertex" selection acceptance, the result is $A = 0.675 \pm 0.010$. We assign a 2% uncertainty to the

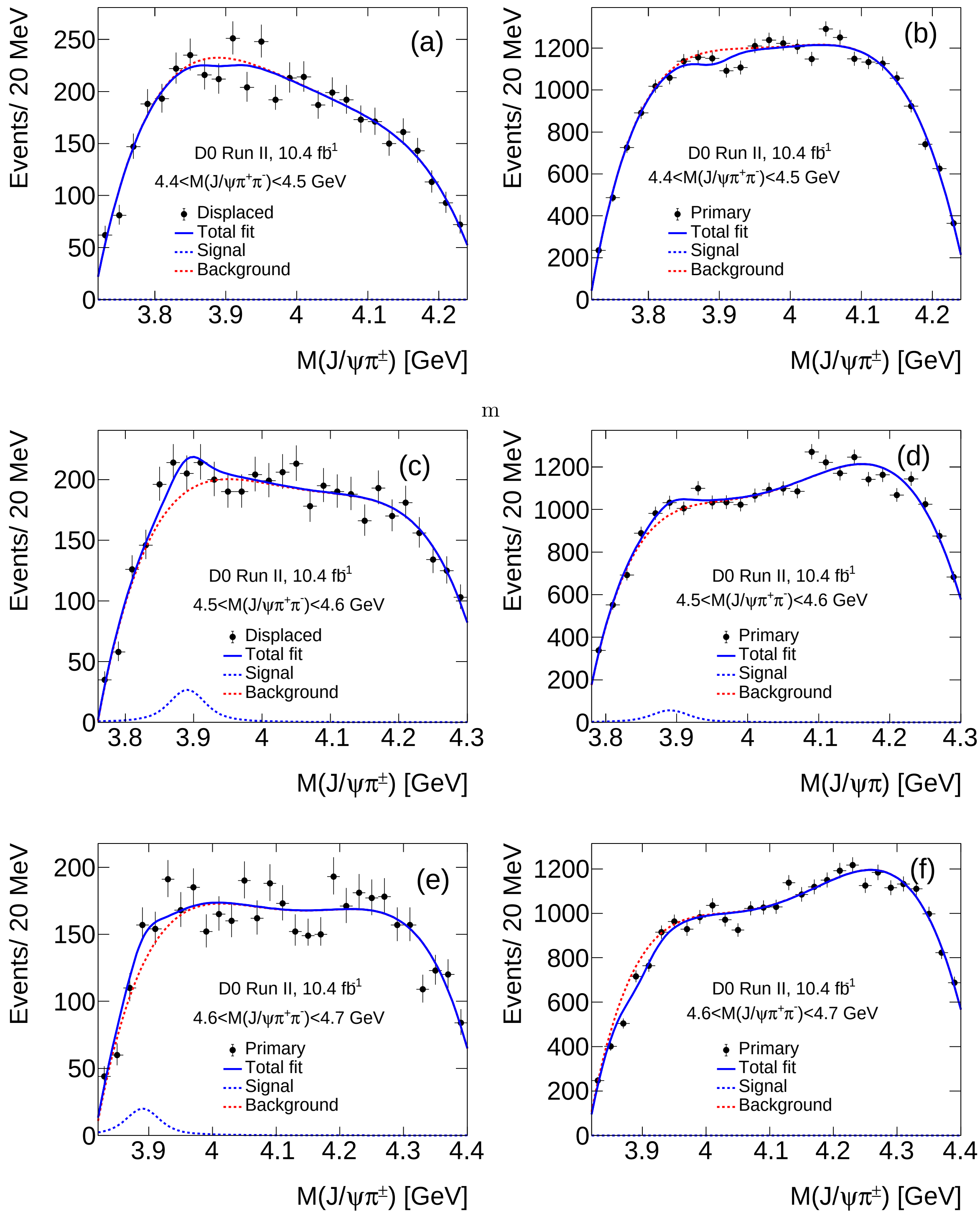

FIG. 3: The invariant mass distribution of $J/\psi\pi^{\pm}$ candidates in three intervals of $M(J/\psi\pi^{+}\pi^{-})$, from top to bottom 4.4–4.5 GeV, 4.5–4.6 GeV, and 4.6–4.7 GeV. Left: events with a displaced vertex. Right: "primary vertex" events. Superimposed are the fits of a Breit-Wigner signal with fixed mass and width [16] (dashed blue lines), a Chebyshev polynomial background (dashed red lines), and their sum (solid blue lines).

displaced-vertex acceptance to account for the differences between the B_d^0 decay and H_b decays.

- Signal model

We vary the fixed parameters [16] of the signal mass and width by ± 2.7 MeV and ± 6.5 MeV, respectively, corresponding to $\pm 1\sigma$.

TABLE I: The $Z_c^{\pm}(3900)$ signal yields, fit quality, and statistical significance S in intervals of $M(J/\psi\pi^+\pi^-)$ for events with a displaced decay vertex and for the complementary sample of "primary vertex" events, using the mass and width fixed at the PDG average values for the $J/\psi\pi^{\pm}$ channel: $M = 3893.3$ MeV, $\Gamma = 36.8$ MeV.

	Displaced vertex			Primary vertex		
$M(J/\psi\pi^+\pi^-)$ GeV	Event yield	χ^2/ndf	S (σ)	Event yield	χ^2/ndf	S (σ)
4.1–4.2	86 ± 68	18.7/14	1.3	-134 ± 144	52.7/15	0.9
4.2–4.3	376 ± 76	28.1/16	5.2	149 ± 203	21.9/14	0.5
4.3–4.4	-148 ± 64	17.4/15	2.3	194 ± 174	16.7/19	1.1
4.4–4.5	-33 ± 60	26.6/15	0.5	-256 ± 170	30.9/18	1.5
4.5–4.6	105 ± 64	23.7/25	1.7	223 ± 162	42.3/23	1.4
4.6–4.7	76 ± 55	57.4/25	1.4	-384 ± 174	46.3/23	2.2

TABLE II: Systematic uncertainties in the $Z_c^{\pm}(3900)$ mass and width measurements for Fig. 5.

Source	Mass, MeV	Width, MeV
Mass calibration	$^{+3}_{-0}$	0
Mass resolution	± 0.1	± 7
Background shape	± 1.4	$^{+25}_{-0}$
Total (sum in quadrature)	$^{+3.3}_{-1.4}$	$^{+26}_{-7}$

- Background shape

  For the "displaced vertex" selection, we assign a symmetric uncertainty based on the differences between the results obtained using the 3rd, 4th, and 5th order polynomial. For the "primary vertex" selection, we assign an asymmetric uncertainty equal to the difference in the results using the 5th-order and 4th-order polynomial. The systematic uncertainties in the signal yield are summarized in Table III.

TABLE III: Systematic uncertainties in the $Z_c^{\pm}(3900)$ signal yield for events in the $4.2 < M(J/\psi\pi^+\pi^-) < 4.3$ GeV interval (Fig.2c and 2d).

Source	Displaced vertex	Primary vertex
Mass resolution	± 18	± 18
Trigger bias	± 19	–
Acceptance	± 7	–
Signal mass	± 11	± 55
Signal width	± 40	± 30
Background shape	± 2	$^{+0}_{-149}$
Total (sum in quadrature)	± 49	$^{+65}_{-163}$

VII. EXTRACTING LIMITS ON PROMPT PRODUCTION RATES

Using results of the mass fits to the "displaced-vertex" and "primary vertex" subsamples and the above value of the acceptance of the displaced vertex selection, we can obtain acceptance-corrected yields of prompt and non-prompt production and their ratio. We determine the yield for the $J/\psi\pi^+\pi^-$mass range 4.2–4.3 GeV where the nonprompt signal is statistically significant.

The mass spectrum in the range 4.2–4.3 GeV in the "primary vertex" category shows no clear $Z_c^{\pm}(3900)$ signal and a large background of about 5000±70 events in the signal region. While there is no visible signal, we cannot exclude a yield comparable to the nonprompt signal.

In calculating the prompt-to-nonprompt ratio, we first obtain the total yield of the nonprompt production by dividing $N_{\rm displaced}$ by the acceptance A. That gives $N_{\rm nonprompt} = 570 \pm 137$ (stat + syst).

Of the above number, a fraction equal to $1 - A$ falls into the "primary vertex" category and must be subtracted to obtain the net number of prompt events, $N_{\rm prompt} = 149 - (1 - 0.66) \times 570 = -45 \pm 237$. In calculating the uncertainty on the total prompt yield, we add the statistical and the systematic uncertainty components in quadrature. We obtain the ratio $r = N_{\rm prompt}/N_{\rm nonprompt} = -0.08^{+0.38}_{-0.46}$. Assuming Gaussian uncertainties and setting the Bayesian prior for negative values of r to zero, we obtain an upper limit of 0.70 at the 95% credibility level.

VIII. SUMMARY AND CONCLUSIONS

Using the D0 Run II data reconstructed with a dedicated extended-tracking algorithm optimized for low-p_T tracks, we have studied production of the exotic state $Z_c^{\pm}(3900)$ in the decays of b hadrons to a $J/\psi\pi^+\pi^-$ system with a subsequent decay to $Z_c^{\pm}(3900)\pi^{\mp}$. The observation is consistent with the sequential decay of a b-

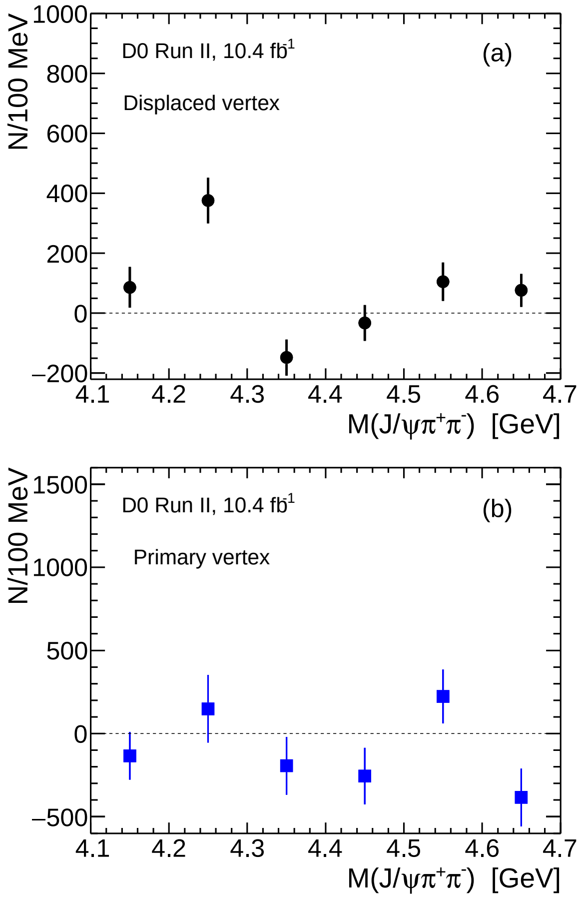

FIG. 4: The $Z_c^+(3900)$ signal yield per 100 MeV for the six intervals of $m(J/\psi\pi^+\pi^-)$: 4.1–4.2, 4.2–4.3, 4.3–4.4, 4.4–4.5, 4.5–4.6 and 4.6–4.7 GeV for (a) "displaced vertex" and (b) "primary vertex" selection. The points are placed at the bin centers.

flavored hadron $H_b \to \psi(4260)$ + anything, $\psi(4260) \to Z_c^{\pm}(3900)\pi^{\mp}$, $Z_c^{\pm}(3900) \to J/\psi\pi^{\pm}$. We find a $Z_c^{\pm}(3900)$ signal at a statistical significance of 5.4σ for events with $4.2 < M(J/\psi\pi^+\pi^-) < 4.3$ GeV, and find its mass and width to be $M = 3902.6^{+5.2}_{-5.0}\,(\text{stat})^{+3.3}_{-1.4}\,(\text{syst})$ MeV and $\Gamma = 32^{+28}_{-21}\,(\text{stat})^{+26}_{-7}\,(\text{syst})$ MeV in agreement with world average values [13, 16].

We searched for evidence of the prompt production of $\psi(4260)$ with subsequent rapid decays to $Z_c^{\pm}(3900)\pi^{\mp}$. In the absence of a significant signal we set an upper limit at the 95% credibility level on the ratio of prompt to nonprompt production, $N_{\text{prompt}}/N_{\text{nonprompt}} < 0.70$. This upper limit is significantly lower than that observed for $X(3872)$, for which $N_{\text{prompt}}/N_{\text{nonprompt}}$ is in the range two to three [3, 4], and $X(4140)$, for which $N_{\text{prompt}}/N_{\text{nonprompt}} \approx 1.5$ [5].

This document was prepared by the D0 collaboration using the resources of the Fermi National Accelerator Laboratory (Fermilab), a U.S. Department of Energy, Office of Science, HEP User Facility. Fermilab is managed by Fermi Research Alliance, LLC (FRA), acting under Contract No. DE-AC02-07CH11359.

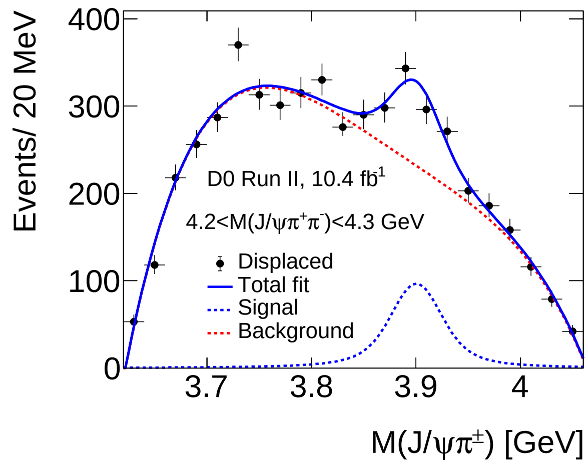

FIG. 5: The $J/\psi\pi^{\pm}$ invariant mass distribution for the "displaced-vertex" candidates at $4.2 < M(J/\psi\pi^+\pi^-) < 4.3$ GeV. The signal (solid blue line) is modeled with a relativistic Breit-Wigner function with free mass and width. Background (dashed red line) is parametrized as a 4th order Chebyshev polynomial.

We thank the staffs at Fermilab and collaborating institutions, and acknowledge support from the Department of Energy and National Science Foundation (United States of America); Alternative Energies and Atomic Energy Commission and National Center for Scientific Research/National Institute of Nuclear and Particle Physics (France); Ministry of Education and Science of the Russian Federation, National Research Center "Kurchatov Institute" of the Russian Federation, and Russian Foundation for Basic Research (Russia); National Council for the Development of Science and Technology and Carlos Chagas Filho Foundation for the Support of Research in the State of Rio de Janeiro (Brazil); Department of Atomic Energy and Department of Science and Technology (India); Administrative Department of Science, Technology and Innovation (Colombia); National Council of Science and Technology (Mexico); National Research Foundation of Korea (Korea); Foundation for Fundamental Research on Matter (The Netherlands); Science and Technology Facilities Council and The Royal Society (United Kingdom); Ministry of Education, Youth and Sports (Czech Republic); Bundesministerium für Bildung und Forschung (Federal Ministry of Education and Research) and Deutsche Forschungsgemeinschaft (German Research Foundation) (Germany); Science Foundation Ireland (Ireland); Swedish Research Council (Sweden); China Academy of Sciences and National Natural Science Foundation of China (China); and Ministry of Education and Science of Ukraine (Ukraine).

[1] S. Chatrchyan *et al.* (CMS Collaboration), "J/ψ and $\psi(2S)$ production in pp collisions at $\sqrt{s} = 7$ TeV", JHEP 02, 011, (2012).

[2] V. M. Abazov *et al.* (D0 Collaboration). "Observation and properties of the $X(3872)$ decaying to $J/\psi\pi^+\pi^-$ in $p\bar{p}$ collisions at $\sqrt{s} = 1.96$ TeV", Phys. Rev. Lett. **93**, 162002, (2004). See also the preliminary result "The "lifetime" distribution of $X(3872)$ mesons produced in $p\bar{p}$ collisions at CDF", CDF note 7159 (2004), https://www-cdf.fnal.gov/physics/new/bottom /051020.blessed-X3872.

[3] S. Chatrchyan *et al.* (CMS Collaboration), "Measurement of the $X(3872)$ production cross section via decays to $J/\psi\pi^+\pi^-$ in pp collisions at $\sqrt{s} = 7$ TeV", JHEP 04, 154 (2013).

[4] M. Aaboud *et al.*, (ATLAS Collaboration), "Measurements of $\psi(2S)$ and $X(3872) \to J/\psi\pi^+\pi^-$ production in pp collisions at $\sqrt{s} = 8$ TeV with the ATLAS detector", JHEP 01, 117 (2017).

[5] V. M. Abazov *et al.* (D0 Collaboration), "Inclusive production of the $X(4140)$ state in $p\bar{p}$ collisions at D0", Phys. Rev. Lett. **115**, 232001 (2015).

[6] E. Braaten, L. He, K. Ingles, "Predictive Solution to the $X(3872)$ Collider Production Puzzle", arXiv:1811.08876 [hep-ph].

[7] V. M. Abazov *et al.* (D0 Collaboration), "Evidence for $Z_c(3900)$ in semi-inclusive decays of $\boldsymbol{b}$-flavored hadrons", Phys. Rev. D **98**, 052010 (2018).

[8] The impact parameter IP is defined as the distance of closest approach of the track to the $p\bar{p}$ collision point projected onto the plane transverse to the $p\bar{p}$ beams.

[9] V. M. Abazov *et al.* (D0 Collaboration), "The upgraded D0 detector", Nucl. Instrum. Methods Phys. Res. A **565**, 463 (2006).

[10] R. Angstadt *et al.*, "The layer 0 inner silicon detector of the D0 experiment", Nucl. Instrum. Methods Phys. Res. A **622**, 278 (2010).

[11] $\eta = -\ln[\tan(\theta/2)]$ is the pseudorapidity and θ is the polar angle between the track momentum and the proton beam direction. ϕ is the azimuthal angle of the track.

[12] V. M. Abazov *et al.* (D0 Collaboration), "The muon system of the Run II D0 detector", Nucl. Instrum. Methods Phys. Res. A **552**, 372 (2005).

[13] M. Tanabashi *et al.* (Particle Data Group), Phys. Rev. D **98**, 030001 (2018).

[14] Z. Q. Liu *et al.* (Belle Collaboration), "Study of $e^+e^- \to \pi^+\pi^- J/\psi$ and Observation of a Charged Charmonium-like State at Belle", Phys. Rev. Lett. **110**, 252002 (2013).

[15] M. Ablikim *et al.* (BESIII Collaboration), "Observation of a Charged Charmoniumlike Structure in $e^+e^- \to \pi^+\pi^- J/\psi$ at $\sqrt{s}$=4.26 GeV", Phys. Rev. Lett. **110**, 252001 (2013).

[16] Ref. [13] lists the $Z_c(3900)$ as a two-channel resonance and quotes average mass for the decays $Z_c(3900) \to D\bar{D}^*$ and $Z_c(3900)^{\pm,0} \to J/\psi\pi^{\pm,0}$. The mass values measured in the two channels differ by 11 MeV and the compatibility is $\approx 4\times10^{-6}$. We choose to calculate the average mass and width for the $J/\psi\pi^\pm$ channel only, using the PDG prescription for measurement averaging.

[17] Cavanaugh, J. E., "Unifying the derivations of the Akaike and corrected Akaike information criteria", Statistics and Probability Letters, **33**, 201 (1997), https://www.sciencedirect.com/science/article/pii/ S0167715296001289?via%3Dihub.